

# Fossilized Nuclei and Chromosomes Reveal 180 Million Years of Genomic Stasis in Royal Ferns

Benjamin Bomfleur,<sup>1\*</sup> Stephen McLoughlin,<sup>1\*</sup> Vivi Vajda<sup>2</sup>

Rapidly permineralized fossils can provide exceptional insights into the evolution of life over geological time. Here, we present an exquisitely preserved, calcified stem of a royal fern (Osmundaceae) from Early Jurassic lahar deposits of Sweden in which authigenic mineral precipitation from hydrothermal brines occurred so rapidly that it preserved cytoplasm, cytosol granules, nuclei, and even chromosomes in various stages of cell division. Morphometric parameters of interphase nuclei match those of extant Osmundaceae, indicating that the genome size of these reputed “living fossils” has remained unchanged over at least 180 million years—a paramount example of evolutionary stasis.

Royal ferns (Osmundaceae) are a basal group of leptosporangiate ferns that have undergone little morphological and anatomical change since Mesozoic times (1–6). Well-preserved fossil plants from 220-million-year-old rocks already exhibit the distinctive architecture of the extant interrupted fern (*Osmunda claytoniana*) (2), and many permineralized os-

mundaceous rhizomes from the Mesozoic are practically indistinguishable from those of modern genera (3–5) or species (6). Furthermore, with the exception of one natural polyploid hybrid (7), all extant Osmundaceae have an invariant and unusually low chromosome count (7, 8), suggesting that the genome structure of these ferns may have remained unchanged over long periods

of geologic time (8). To date, evidence for evolutionary conservatism in fern genomes has been exclusively based on studies of extant plants (9, 10). Here, we present direct paleontological evidence for long-term genomic stasis in this family in the form of a calcified osmundaceous rhizome from the Lower Jurassic of Sweden with pristinely preserved cellular contents, including nuclei and chromosomes.

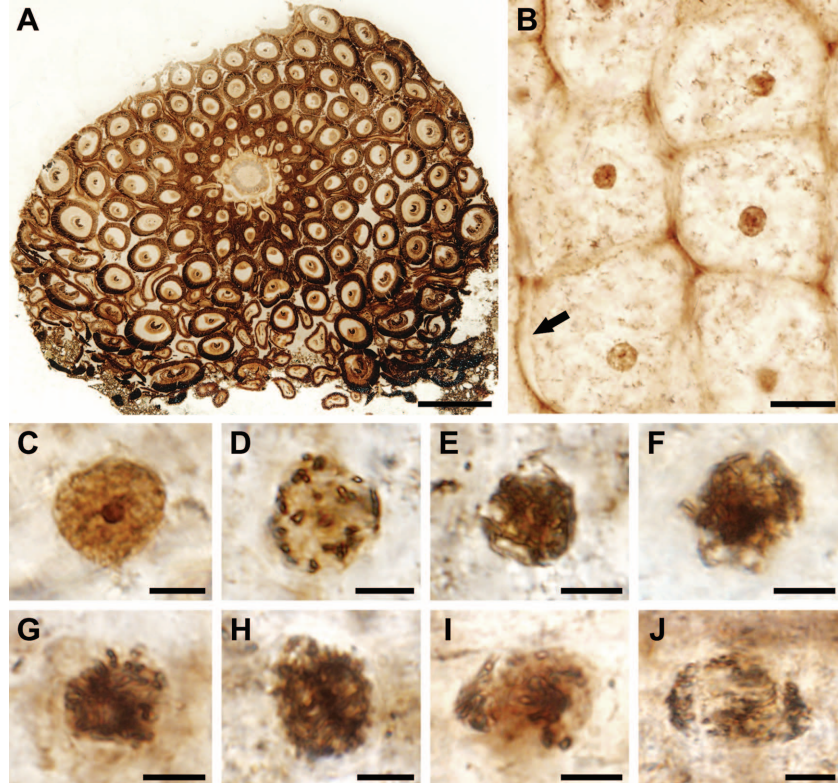
The specimen was collected from mafic volcaniclastic rocks [informally named the “Djupadal formation” (11)] at Korsaröd near Höör, Scania, Sweden [fig. S1 of (12)]. Palynological analysis indicates an Early Jurassic (Pliensbachian) age for these deposits (11) (fig. S2), which agrees with radiometric dates obtained from nearby volcanic necks (13) from which the basaltic debris originated. The fern rhizome was permineralized *in vivo* by calcite from hydrothermal brines (11, 14) that per-

<sup>1</sup>Department of Palaeobiology, Swedish Museum of Natural History, Post Office Box 50007, SE-104 05 Stockholm, Sweden.

<sup>2</sup>Department of Geology, Lund University, Sölvegatan 12, SE-223 62 Lund, Sweden.

\*Corresponding author. E-mail: benjamin.bomfleur@nrm.se (B.B.); steve.mcloughlin@nrm.se (S.M.)

**Fig. 1. Cytological features preserved in the apical region of the Korsaröd fern fossil.** (A) transverse section through the rhizome; (B) detail of radial longitudinal section showing typical pith–parenchyma cells with preserved cell membranes (arrow), cytoplasm and cytosol particles, and interphase nuclei with prominent nucleoli; (C) interphase nucleus with nucleolus and intact nuclear membrane; (D) early prophase nucleus with condensing chromatin and disintegrating nucleolus and nuclear membrane; (E and F) late prophase cells with coiled chromosomes and with nucleolus and nuclear membrane completely disintegrated; (G and H) prometaphase cells showing chromosomes aligning at the equator of the nucleus; (I and J) possible anaphase cells showing chromosomes attenuated toward opposite poles. (A), (C to E), (G), and (I) are from NRM S069656. (B), (F), (H), and (J) are from NRM S069658. Scale bars: (A) 500 μm; (B) 20 μm; (C to J) 5 μm.



colated through the coarse-grained sediments shortly after deposition (table S1). The fossil is 6 cm long and 4 cm wide and consists of a small (~7 mm diameter) central stem surrounded by a dense mantle of persistent frond bases with interspersed rootlets (Fig. 1). Its complex reticulate vascular cylinder (ectophloic dictyoxyllic siphonostele), parenchymatous pith and inner cortex, and thick fibrous outer cortex are characteristic features of Osmundaceae (1, 3–5, 12) (fig. S3). Moreover, the frond bases mantling the rhizome contain a heterogeneous sclerenchyma ring that is typical of extant *Osmunda* sensu lato (1, 3, 4, 12) (fig. S4). The presence of a single root per leaf trace favors affinities with (sub)genus *Osmundastrum* (1, 3, 6, 12).

The specimen is preserved in exquisite subcellular detail (Fig. 1 and figs. S4 and S5). Parenchyma cells in the pith and cortex show preserved cell contents, including membrane-bound cytoplasm, cytosol granules, and possible amyloplasts (Fig. 1 and fig. S5). Most cells contain interphase nuclei with conspicuous nucleoli (Fig. 1, figs. S4 and S5, and movies S1 and S2). Transverse and longitudinal sections through the apical part of the stem also reveal sporadic dividing parenchyma cells, mainly in the pith periphery (Fig. 1). These are typically preserved in prophase or telophase stages, in which the nucleolus and nuclear envelope are more or less unresolved and the chromatin occurs in the form of diffuse, granular material or as distinct chromatid strands. A few

cells contain chromosomes that are aligned at the equator of the nucleus, indicative of early metaphase, and two cells were found to contain chromosomes that appear to be attenuated toward opposite poles, representing possible anaphase stages. Some tissue portions in the stem cortex and the outer leaf bases show signs of necrosis and programmed cell death (fig. S6).

Such fine subcellular detail has rarely been documented in fossils (15–17) because the chances for fossilization of delicate organelles are small (16) and their features are commonly ambiguous (17). The consistent distribution and architecture of the cellular contents in the Korsaröd fern fossil resolved via light microscopy (Fig. 1 and fig. S4), scanning electron microscopy (fig. S5), and synchrotron radiation x-ray tomographic microscopy (SRXTM) (fig. S5 and movies S1 and S2) provide unequivocal evidence for three-dimensionally preserved organelles.

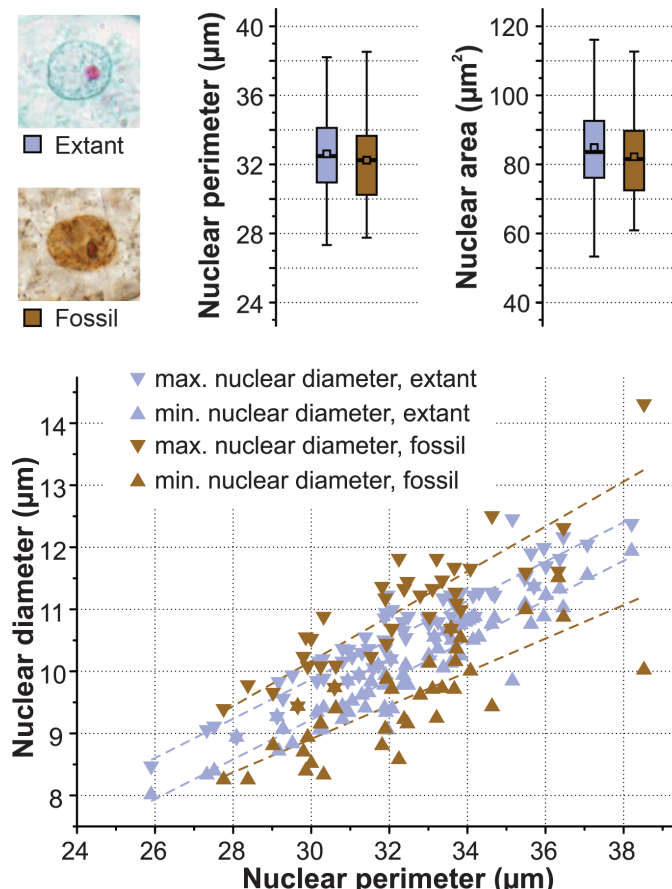
Positive scaling relationships rooted in DNA content can be used to extrapolate relative genome sizes and ploidy levels of plants (18–21). We measured minimum and maximum diameters, perimeters, and maximum cross-sectional areas of interphase nuclei in pith and cortical parenchyma cells of the fossil and of its extant relative *Osmundastrum cinnamomeum*. The measurements match very closely (Fig. 2), with mean nuclear perimeters of 32.2 versus 32.6  $\mu\text{m}$  and mean areas of 82.2 versus 84.9  $\mu\text{m}^2$  in the fossil

and in extant *Osmundastrum*, respectively. The equivalent nuclear sizes demonstrate that the Korsaröd fern fossil and extant Osmundaceae likely share the same chromosome count and DNA content, and thus suggest that neither ploidization events nor notable amounts of gene loss have occurred in the genome of the royal ferns since the Early Jurassic ~180 million years ago [(8), see also discussion in (9, 10)]. These results, in concert with morphological and anatomical evidence (1–6), indicate that the Osmundaceae represents a notable example of evolutionary stasis among plants.

#### References and Notes

- W. Hewitson, *Ann. Mo. Bot. Gard.* **49**, 57–93 (1962).
- C. Phipps et al., *Am. J. Bot.* **85**, 888–895 (1998).
- C. N. Miller, *Contrib. Mus. Paleontol.* **23**, 105–169 (1971).
- G. W. Rothwell, E. L. Taylor, T. N. Taylor, *Am. J. Bot.* **89**, 352–361 (2002).
- N. Tian, Y.-D. Wang, Z.-K. Jiang, *Palaeoworld* **17**, 183–200 (2008).
- R. Serbet, G. W. Rothwell, *Int. J. Plant Sci.* **160**, 425–433 (1999).
- C. Tsutsumi, S. Matsumoto, Y. Yatabe-Kakugawa, Y. Hirayama, M. Kato, *Syst. Bot.* **36**, 836–844 (2011).
- E. J. Klekowski, *Am. J. Bot.* **57**, 1122–1138 (1970).
- M. S. Barker, P. G. Wolf, *Bioscience* **60**, 177–185 (2010).
- I. J. Leitch, A. R. Leitch, in *Plant Genome Diversity*, I. J. Leitch, J. Greilhuber, J. Doležel, J. F. Wendel, Eds. (Springer-Verlag, Wien, 2013), vol. 2, pp. 307–322.
- C. Augustsson, *GFF* **123**, 23–28 (2001).
- See supplementary materials available on Science Online.
- I. Bergelin, *GFF* **131**, 165–175 (2009).
- A. Ahlberg, U. Sivhed, M. Erlström, *Geol. Surv. Denm. Greenl. Bull.* **1**, 527–541 (2003).
- S. D. Brack-Hanes, J. C. Vaughn, *Science* **200**, 1383–1385 (1978).
- K. J. Niklas, *Am. J. Bot.* **69**, 325–334 (1982).
- J. W. Hagadorn et al., *Science* **314**, 291–294 (2006).
- A. E. DeMaggio, R. H. Wetmore, J. E. Hannaford, D. E. Stettler, V. Raghavan, *Bioscience* **21**, 313–316 (1971).
- J. Masterson, *Science* **264**, 421–424 (1994).
- I. Símová, T. Herben, *Proc. Biol. Sci.* **279**, 867–875 (2012).
- B. H. Lomax et al., *New Phytol.* **201**, 636–644 (2014).

**Fig. 2. Morphometric parameters of interphase nuclei of extant *O. cinnamomeum* compared to those of the Korsaröd fern fossil.** Colored box-and-whiskers plots in upper graph indicate interquartile ranges (box) with mean (square), median (solid transverse bar), and extrema (whiskers); dashed colored lines in lower graph indicate linear fits ( $n = 76$  versus  $n = 37$ ) measured nuclei for extant *O. cinnamomeum* versus the fossil.



**Acknowledgments:** We thank E. M. Friis and S. Bengtsson (Stockholm) and F. Marone and M. Stamparoni (Villigen) for assistance with SRXTM analyses at the Swiss Light Source, Paul Scherrer Institute (Villigen); G. Grimm (Stockholm) for assistance with statistical analyses; B. Bremer and G. Larsson (Stockholm) for providing live material of *Osmunda*; M. A. Gandolfo Nixon and J. L. Svitko (Ithaca, New York) for permission to use images from the Cornell University Plant Anatomy Collection (CUPAC; <http://cupac.bh.cornell.edu/>); the members of Tjörnarps Sockengille (Tjörnarp) for access to the fossil locality; A.-L. Decombeix (Montpellier), I. Bergelin (Lund), C. H. Haftor (Lawrence, Kansas), N. Tian (Shenyang), Y.-D. Wang (Nanjing), and T. E. Wood (Flagstaff, Arizona) for discussion; and two anonymous referees for constructive comments. This research was jointly supported by the Swedish Research Council (VR), Lund University Carbon Cycle Centre (LUCC), and the Royal Swedish Academy of Sciences. The material is curated at the Swedish Museum of Natural History (Stockholm, Sweden) under accession nos. S069649 to S069658 and S089687 to S089693.

#### Supplementary Materials

[www.sciencemag.org/content/343/6177/1376/suppl/DC1](http://www.sciencemag.org/content/343/6177/1376/suppl/DC1)

Materials and Methods

Supplementary Text

Figs. S1 to S6

Table S1

References (22–36)

Movies S1 and S2

17 December 2013; accepted 21 February 2014  
10.1126/science.1249884

## Supplementary Materials for

### **Fossilized Nuclei and Chromosomes Reveal 180 Million Years of Genomic Stasis in Royal Ferns**

Benjamin Bomfleur,\* Stephen McLoughlin,\* Vivi Vajda

\*Corresponding author. E-mail: benjamin.bomfleur@nrm.se (B.B.); steve.mcloughlin@nrm.se (S.M.)

Published 21 March 2014, *Science* **343**, 1376 (2014)  
DOI: 10.1126/science.1249884

**This PDF file includes:**

- Materials and Methods
- Supplementary Text
- Figs. S1 and S6
- Table S1
- Captions for Movies S1 and S2
- References

**Other Supplementary Material for this manuscript includes the following:**  
(available at [www.sciencemag.org/content/343/6177/1376/suppl/DC1](http://www.sciencemag.org/content/343/6177/1376/suppl/DC1))

Movies S1 and S2

## **Materials and Methods:**

Standard 30 µm thin sections (22, 23) of the fossil and of extant *Osmundastrum* were studied with an BX51 compound microscope (Olympus; Vendelsö, Sweden) and photographed using an DP71 digital camera (Olympus). Nuclear parameters were measured using cellSens© Dimension version 1.6 (Olympus Soft Imaging Systems; Münster, Germany), and analysed using Origin© version 8 (OriginLab; Northampton, MA). Transverse and radial longitudinal surfaces of the permineralized rhizome were polished and then etched in 5% HCl for 5–10 seconds; after drying, these specimens were sputter-coated with gold for 90 seconds, and examined and imaged using a S-4300 field emission scanning electron microscope (Hitachi; Krefeld, Germany) at the Swedish Museum of Natural History (Naturhistoriska Riksmuseet). In addition, a portion of a permineralized stipe (petiole) was removed and analysed using synchrotron X-ray tomographic microscopy at the TOMCAT beam-line of the Swiss Light Source, Paul Scherrer Institute (Villigen, Switzerland) [see (24–26)]. The tomographic data were processed and reconstructed using Avizo© Fire version 8 (FEI Visualization Sciences Group; Hillsboro, OR). We applied conventional adjustments of brightness, contrast, and saturation to the digital images using Adobe© Photoshop© CS5 Extended version 12.0 (Adobe Systems Incorporated; San Jose, CA).

Five samples of the host rock (NRM S069690, NRM S069730, NRM S06738, NRM S069740, and NRM S069644) were processed for palynological analysis following the standard methods at Global GeoLab Ltd. (Medicine Hat, Canada). One entire strew slide per sample was analysed for presence/absence data, and 200 palynomorphs per sample were counted for relative abundance data where possible.

Measurements of major and trace elements were obtained using a Niton XL3t Goldd+ X-ray fluorescence (XRF) analyzer (Thermo Scientific; Örebro, Sweden) at the Department of Geology, Lund University; calibration and drift detection was undertaken using standard sample NIST 2709a with known reference values. The volcaniclastic host rock (sample NRM S069645) and a polished surface of the fern fossil (sample NRM S069649) were both analyzed for elemental constituents over target areas of 8 mm diameter. Fossil material (NRM S069649–S069658) and measured slides of extant *Osmundastrum cinnamomeum* (NRM S089694) are housed in the Department of Palaeobiology at the Swedish Museum of Natural History, Stockholm, Sweden.

## **Supplementary Text**

### Palynological dating:

The samples yielded low- to moderate-diversity assemblages of non-marine palynomorphs, including spores, pollen, and fresh-water algae. Abundance data were assessed for samples NRM S069690 and NRM S069730, which are both dominated by fern spores (52% and 63%, respectively) followed by gymnosperm pollen grains (33% and 43%, respectively). Taxa occurring in high relative abundances include the spores *Osmundacidites wellmanii* Couper 1953 (Osmundaceae: up to 12% in sample NRM S069690), *Cyathidites minor* Couper 1953 (Cyatheaceae), *Deltoidospora toralis* (Leschik) Lund 1977 (Matoniaceae, Dicksoniaceae, Cyatheaceae, or Dipteridaceae), and *Marattisporites scabratus* Couper 1958 (Marattiaceae). Gymnosperm pollen grains are

mainly represented by *Perinopollenites elatoides* Couper 1958, *Classopolis* spp., *Alisporites* spp., *Chasmatosporites* spp., and *Eucommiidites troedssonii* Erdtman 1948. Additional taxa include *Striatella seebergensis* Mädler, 1964, *Retitriletes clavatoides* (Cookson 1953) Döring et al. in Krutzsch 1963, *Spheripollenites psilatus* Couper 1958, and a few specimens of *Cerebropollenites thiergartii* Schulz 1967 and *Vitreisporites pallidus* (Reissinger) Nilsson 1958.

The high relative abundance of fern spores, *Chasmatosporites* spp., and *Alisporites* spp. together with the scarcity of *Classopolis* and *Spheripollenites psilatus* and absence of Toarcian key-taxa (e.g., *Clavatipollenites hughesii* and *Callialasporites* spp.) indicate a late Pliensbachian age for the assemblage. The spore-pollen suite correlates with the Sinemurian–Pliensbachian *Cerebropollenites macroverrucosus* Zone (27) and with the Pliensbachian *Chasmatosporites* Zone (28) established in southern Scandinavia. It also closely matches palynofloras from the late Pliensbachian Assemblage Zone 3 (*Chasmatosporites*–*Cerebropollenites thiergartii*–*Botryococcus* Zone) (29) and the late Pliensbachian Assemblage A (A2) (30) established in Greenland.

A further important observation is the unusually common occurrence of large, intact clusters of *Marattisporites scabratus* Couper 1953, indicating a short transport distance for the palynomorphs.

List of taxonomically diagnostic characters of the permineralized fern rhizome (Fig. S3):

- (a) Rhizome radially symmetrical with a dense mantle of leaf bases and rootlets
- (b) Siphonostele, ectophloic-dictyoxyllic
- (c) Pith parenchymatous
- (d) Xylem cylinder thin (<15 tracheids thick), dissected by mostly complete leaf gaps
- (e) Inner cortex thin, parenchymatous; outer cortex thick, homogeneous, fibrous
- (f) Leaf traces endarch, initially oblong to slightly curved with one protoxylem cluster
- (g) Adventitious roots arising singly from each leaf trace
- (h) Stipe-base vascular strand C-shaped, enclosing a mass of thick-walled fibers in its concavity
- (i) Stipe-base sclerenchyma ring heterogeneous, containing thin- and thick-walled fibers

Following systematic treatments of Osmundaceae (1, 3–5),

- (a, b) are diagnostic of family Osmundaceae,
- (b, c) are diagnostic of subfamily Osmundoideae,
- (d–f) are diagnostic of genus *Osmunda* s.l. and of the fossil form-genus *Ashicaulis*,
- (h, i) are diagnostic of genus *Osmunda* s.l.,
- and (g) is typical of subgenus *Osmundastrum*.

Fossils with overall comparable character combinations have been assigned to the form-genus *Ashicaulis* [see (4, 5, 31–34)] or described as fossil representatives of *Osmunda* (e.g., *O. pluma*, *O. arnoldii*, *O. dowkeri*, and fossil *O. cinnamomea*) (3). Preliminary analyses indicate that the studied specimen shows a unique combination of specific anatomical characters, and probably represents a new species.

X-ray fluorescence analysis:

In decreasing abundance, the most common elements detected in the volcaniclastic host rock are Si (36.65%), Fe (26.8%), Al (16.6%), Mg (8.65%), K (6.77%), Ti (2.34%), and Ca (1.47%) indicating a dominance of Fe-, Al- and Mg-silicate minerals in the mafic volcaniclastic matrix (table S1). Other elements constitute < 1% of the rock composition (table S1). Note that the XRF analyser does not detect elements with atomic numbers less than that of Mg, so the registered percentages (table S1) are exclusive of those elements. The composition of the host rock is thus consistent with that of the mafic alkaline magmatic rocks of the central Skåne volcanic province (35). The results from the XRF analysis of the fossil fern, by contrast, show an extremely high value of Ca (91.84%), followed by Si (3.21%) and P (1.96%). The very different compositions of the fossil and rock matrix demonstrate that calcite cement precipitated preferentially around and within the entombed plant remains, which we infer to be a result of contrasting local porosity and chemical environments within and around buried plant tissues.

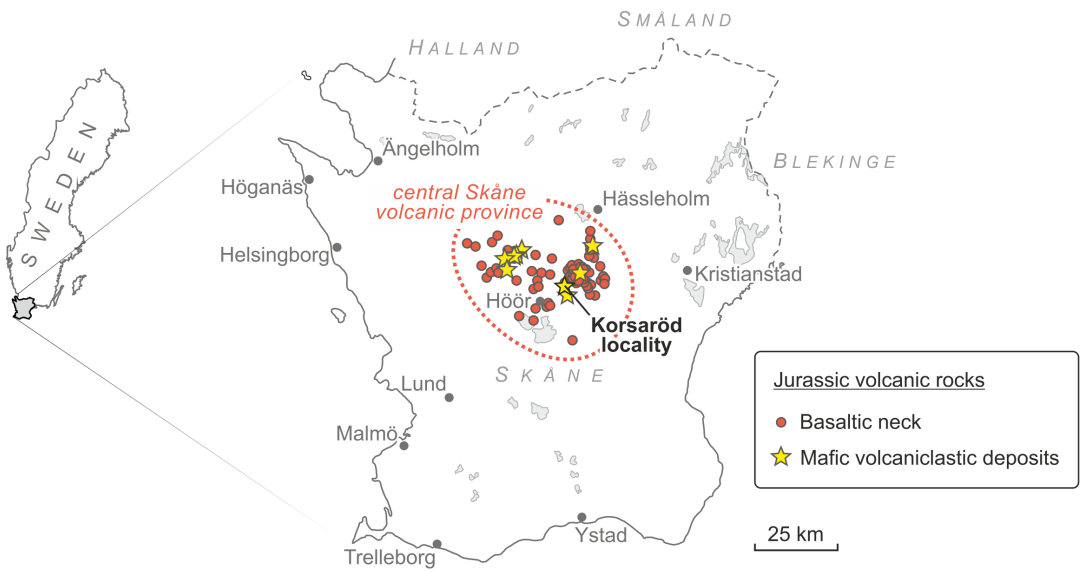


**Fig. S1.**

Map of southern Sweden showing the location of the Korsaröd fossil site in the central Skåne volcanic province.

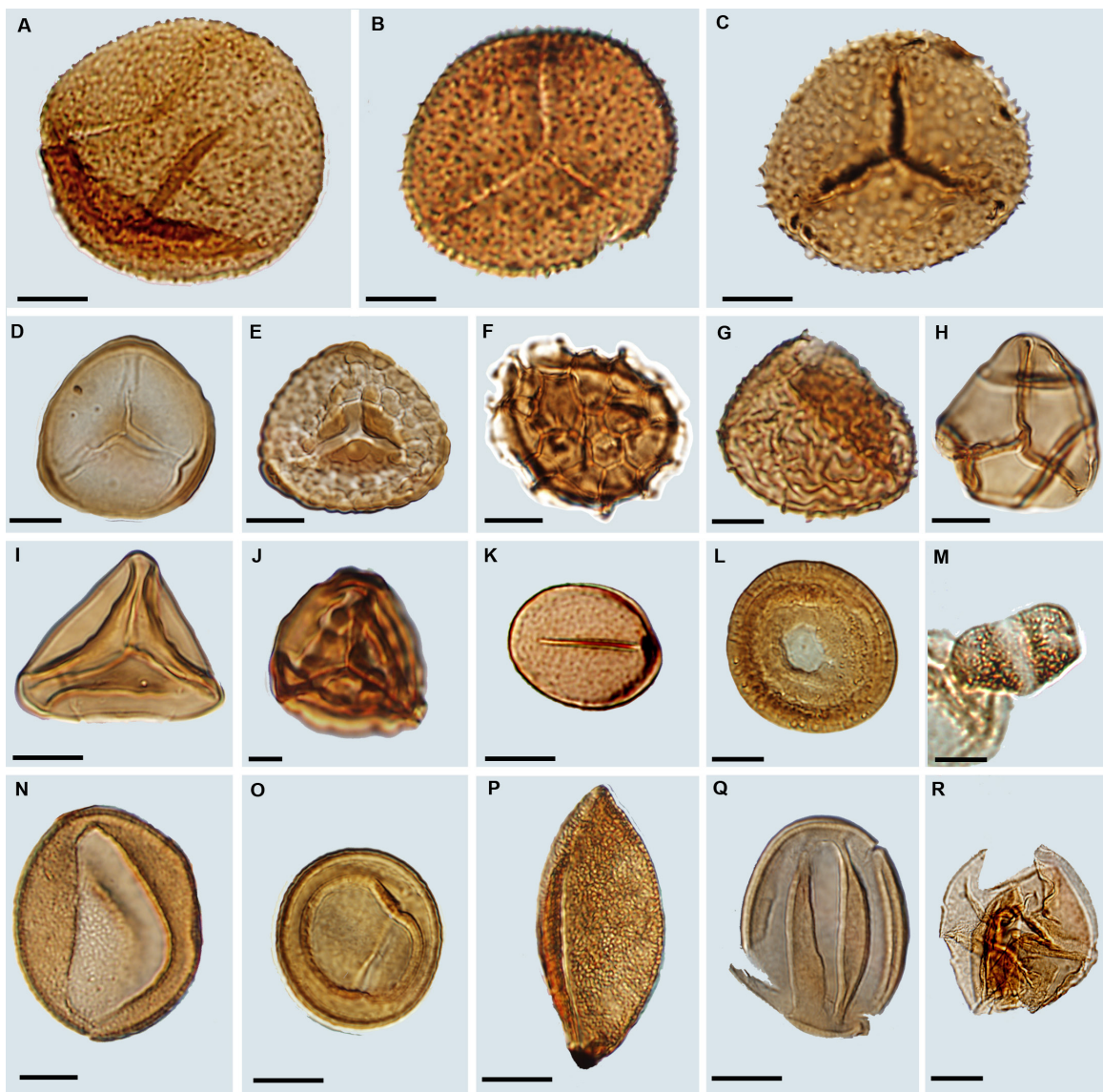


**Fig. S2**

Light micrographs of representative fossil spores and pollen grains from the 'Djupadal formation' at the Korsaröd locality; taxon, rock sample number, palynomorph specimen number, and microscope X/Y calibration position.

(A–C) *Osmundacidites wellmanii* Couper 1953; (A) NRM S069738, NRMS089691-01, 127/15; (B) NRM S069690, NRMS089687-01, 119/7; (C) NRM S069730, NRMS089689-01, 144/17; (D) *Stereisporites psilatus* (Ross) Pflug in Thomson & Pflug 1953, NRM S069690, NRMS089687-02, 137/5; (E) *Stereisporites seebergensis* Schulz 1966, NRM S069730, NRMS089689-02, 132/10; (F) *Retitriletes clavatoides* Döring 1963, NRM S069690, NRMS089687-03, 134/5; (G) *Retitriletes semimuris* (Danze-Corsin & Laveine 1963) McKellar 1974, NRM S069730, NRMS089689-03, 114/18; (H) *Cibotiumspora jurienensis* (Balme) Filatoff 1975, NRM S069690, NRMS089687-04, 113/14; (I) *Deltoidospora toralis* (Leschik) Lund 1977, NRM S069730, NRMS089689-04, 140/20; (J) *Striatella seebergensis* Mädler 1964, NRM S069690, NRMS089687-05,

132/10; (**K**) *Marattisporites scabratus* Couper 1958, NRM S069730, NRMS089689-05, 142/8; (**L**) *Classopollis classoides* (Pflug) Pocock & Jansonius 1961, NRM S069690, NRMS089687-06, 125/15; (**M**) *Vitreisporites pallidus* (Reissinger) Nilsson 1958, NRM S069738, NRMS089691-02, 124/16; (**N**) *Chasmatosporites hians* Nilsson 1958, NRM S069730, NRMS089689-06, 139/18; (**O**) *Chasmatosporites apertus* (Rogalska) Nilsson 1958, NRM S069690, NRMS089687-07, 137/2; (**P**) *Monosulcites punctatus* Orlowska-Zwolinska 1966, NRM S069730, NRMS089689-07, 133/8; (**Q**) *Eucommiidites troedssonii* Erdtman 1948, NRM S069690, NRMS089687-08, 144/15; (**R**) *Perinopollenites elatoides* Couper 1958, NRM S069690, NRMS089687-09, 137/15. Scale bars 10 µm.

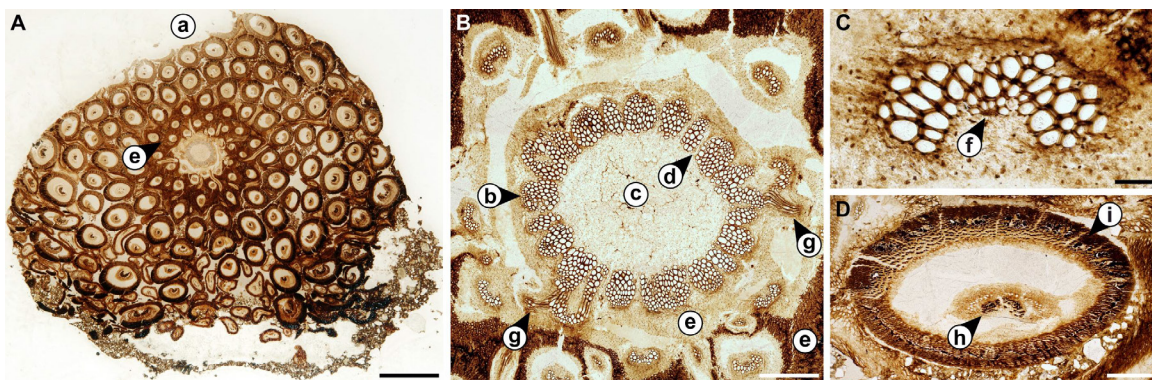


**Fig. S3**

Transmitted-light micrographs illustrating the diagnostic morphological and anatomical features of the Korsaröd fern fossil. **(A)** Transverse section through the radially symmetrical rhizome with a dense mantle of stipe bases and rootlets (a), NRM S069656; **(B)** detail of transverse section through the stem showing the ectophloic-dictyoxyllic siphonostele (b), the parenchymatous pith (c), the thin xylem cylinder dissected by complete gaps (d), the thin parenchymatous inner cortex and fibrous outer cortex (e), and the single root per leaf trace (g), NRM S069656; **(C)** transverse section through an endarch, slightly reniform leaf trace with a single protoxylem cluster (f) in the inner cortex of the stem, NRM S069656; **(D)** transverse section through a stipe base showing the C-shaped leaf trace and enclosed sclerenchyma mass (h) and an arch of thick-walled fibers in the sclerenchyma ring (i), NRM S069657. Scale bars **(A)** 5 mm; **(B, D)** 500 µm; **(C)** 50 µm.

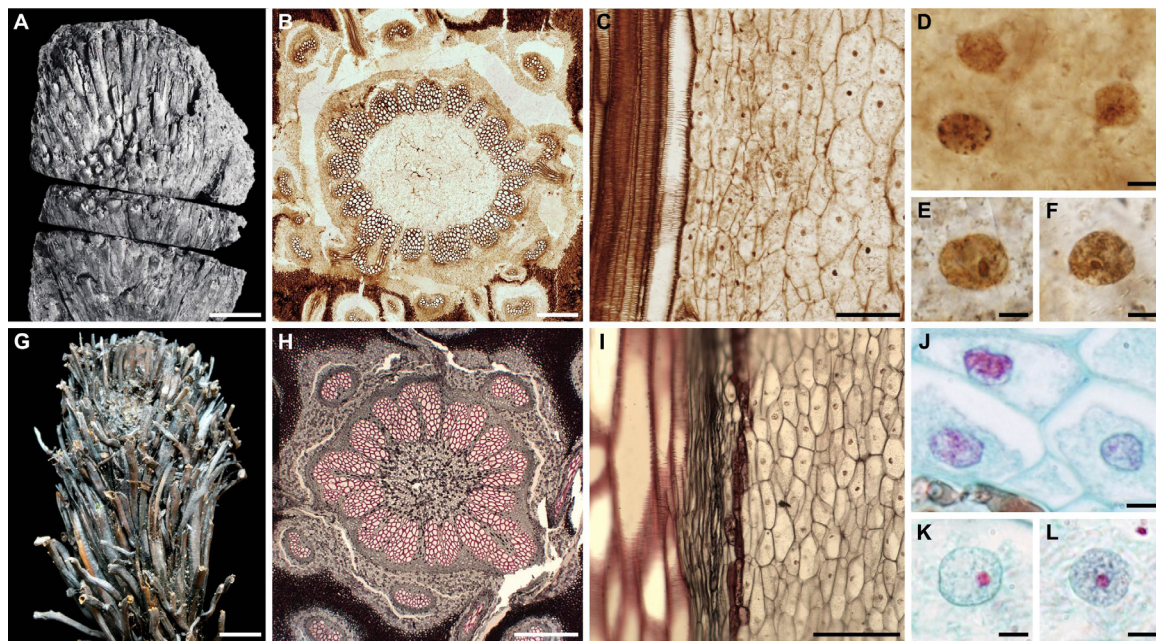


**Fig. S4**

Morphological, anatomical, and cytological features of the Korsaröd fern fossil (A–F) compared to those of extant *Osmunda regalis* (G) and *Osmundastrum cinnamomeum* (H–L). (A, G) Gross morphology of rhizome showing dense mantle of persistent stipe bases and fine roots; (B, H) stem cross sections showing the equivalent ectophloic-dictyoxyllic siphonostele; (C, I) longitudinal sections of stem portions showing xylem cylinder with scalariform-pitted tracheids of the stele (left) and organelle-bearing parenchyma cells of the pith (right); (D, J) details of three cortical parenchyma cells, each containing a nucleus; (E, F, K, L) details of interphase nuclei with intact nuclear membranes and prominent nucleoli. Images H and I used with kind permission of the Cornell University Plant Anatomy Collection (CUPAC; <http://cupac.bh.cornell.edu/>). Fossil specimens: (A) reassembly of original fossil now cut into blocks NRM S069649–S069655; (B) thin section S069656; (C) thin section NRM S069658; (D–E) NRM S069656. (J–L) Thin section of extant *O. cinnamomeum*, NRM S089694. Scale bars (A, G) 1 cm; (B, H) 500 µm; (C, I) 100 µm; (D–F, K–L) 5 µm.

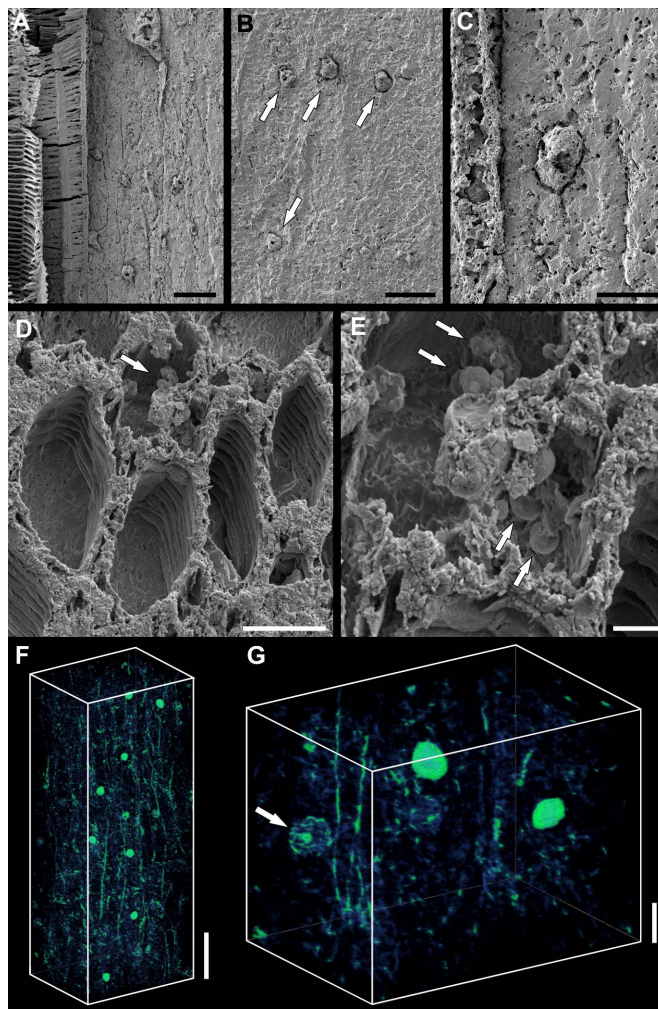


**Fig. S5**

Intracellular details of the Korsaröd fern fossil revealed through SEM of acid-etched surfaces (A–E) and through synchrotron X-ray tomographic microscopy of a stipe portion (F, G). (A) Vascular-bundle tracheids (left), parenchyma cell walls, and preserved nuclei projecting from etched surface of longitudinal section of a stipe, NRM S069655; (B, C) details of etched longitudinal sections through a stipe showing projecting nuclei (arrows in B), NRM S069655; (D, E) etched surface of a transverse section of a stipe showing tracheid cells with characteristic scalariform pitting and an associated parenchyma cell containing putative amyloplasts (arrows), NRM S069649; (F, G) semi-translucent box reconstructions of small portions of cortical parenchyma in a stipe showing distribution of nuclei, some with visible nucleoli (arrow in G; see movies S1, S2), NRM S069654. Scale bars (A, B, D) 25 µm; (C, G) 10 µm; (E) 5 µm; (F) 50 µm.

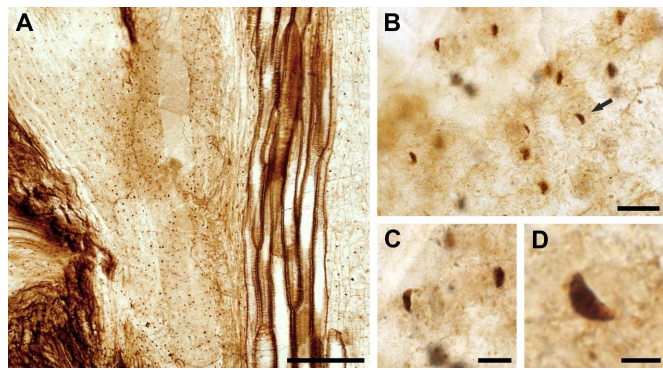


**Fig. S6**

Signs of necrosis and programmed cell death in the Korsaröd fern fossil. (A) Radial longitudinal section through the stem showing (from left to right) cortical tissues, xylem cylinder, and pith, with a darker patch of apparently necrotic tissue in the inner cortex (image center); (B) detail of the same, showing shrunken cytoplasm and pyknotic nuclei (arrow) typical of apoptosis (36); (C, D) details showing pyknotic nuclei containing homogeneous nuclear contents condensed into a distinctive dark crescent at one pole of the former nuclear envelope. All images from NRM S069658. Scale bars (A) 500 µm; (B) 40 µm; (C) 10 µm; (D) 5 µm.

**Table S1**

Results of X-ray fluorescence analysis of the volcaniclastic host rock and the fern fossil from the Korsaröd site, showing the proportions of major (bold font), minor (regular font) and trace (gray) elemental components.

Fern fossil		Sedimentary matrix		
	NRMS069749, Ø 8 mm (ppm)	Instrument error (%)	NRMS069645, Ø 8 mm (ppm)	Instrument error (%)
<b>Ca</b>	<b>367,868.0</b>	0.5	9,051.9	4.8
Si	12,820.9	5.65	<b>221,165.9</b>	0.7
P	7,994.4	4.2	3,176.6	7.9
Al	3,339.6	60.8	<b>104,738.0</b>	3.2
Cl	1,992.8	5.2	301.1	19.0
S	1,831.4	8.1	2,074.5	4.5
Ti	1,431.2	8.2	14,484.0	1.4
K	1,173.4	12.2	41,743.8	1.4
Sr	602.5	1.0	37.8	4.9
Ba	330.9	9.8	968.5	4.3
W	171.5	17.8	245.4	16.2
Ni	142.0	15.7	491.9	7.2
Cu	92.8	11.6	184.1	9.0
Zr	74.7	4.3	125.8	2.9
Y	68.1	3.4	38.5	7.5
Cs	63.4		20.7	
Mn	63.3	3.6	849.2	9.2
Fe	55.5	2.7	<b>166,180.3</b>	0.6
V	34.1	40.8	533.7	14.1
Hg	28.9	20.5	-	-
Zn	25.3	21.5	114.6	10.0
Co	16.9	60.5	-	-
Au	8.8	57.5	-	-
Rb	5.1	23.6	79.5	3.1
As	5.0	31.7	-	-
Nb	4.0	33.2	30.4	6.9
Mg	-	-	61,187.0	15.0
Cr	-	-	1,261.1	4.6

**Movie S1**

Conventional tomographic reconstruction of a cuboidal portion of stipe parenchyma from the Korsaröd fern fossil showing cell walls and distribution of nuclei. Note nucleoli, e.g., within a nucleus in the upper left corner of the box after *ca*  $\frac{1}{4}$  rotation.

**Movie S2**

Red-cyan stereoscopic tomographic reconstruction of the same.

## References and Notes

1. W. Hewitson, Comparative morphology of the Osmundaceae. *Ann. Mo. Bot. Gard.* **49**, 57–93 (1962). [doi:10.2307/2394741](https://doi.org/10.2307/2394741)
2. C. Phipps, T. Taylor, E. Taylor, R. Cúneo, L. Boucher, X. Yao, Osmunda (Osmundaceae) from the Triassic of Antarctica: An example of evolutionary stasis. *Am. J. Bot.* **85**, 888–895 (1998). [Medline](#) [doi:10.2307/2446424](https://doi.org/10.2307/2446424)
3. C. N. Miller, *Contrib. Mus. Paleontol.* **23**, 105–169 (1971).
4. G. W. Rothwell, E. L. Taylor, T. N. Taylor, *Ashicaulis woolfei* n. sp.: Additional evidence for the antiquity of osmundaceous ferns from the Triassic of Antarctica. *Am. J. Bot.* **89**, 352–361 (2002). [Medline](#) [doi:10.3732/ajb.89.2.352](https://doi.org/10.3732/ajb.89.2.352)
5. N. Tian, Y.-D. Wang, Z.-K. Jiang, Permineralized rhizomes of the Osmundaceae (Filicales): Diversity and tempo-spatial distribution pattern. *Palaeoworld* **17**, 183–200 (2008). [doi:10.1016/j.palwor.2008.10.004](https://doi.org/10.1016/j.palwor.2008.10.004)
6. R. Serbet, G. W. Rothwell, *Osmunda cinnamomea* (Osmundaceae) in the Upper Cretaceous of Western North America: Additional Evidence for Exceptional Species Longevity among Filicalean Ferns. *Int. J. Plant Sci.* **160**, 425–433 (1999). [doi:10.1086/314134](https://doi.org/10.1086/314134)
7. C. Tsutsumi, S. Matsumoto, Y. Yatabe-Kakugawa, Y. Hirayama, M. Kato, A New Allotetraploid Species of *Osmunda* (Osmundaceae). *Syst. Bot.* **36**, 836–844 (2011). [doi:10.1600/036364411X604859](https://doi.org/10.1600/036364411X604859)
8. E. J. Klekowski, Populational and genetic studies of a homosporous fern-Osmunda regalis. *Am. J. Bot.* **57**, 1122–1138 (1970). [doi:10.2307/2441278](https://doi.org/10.2307/2441278)
9. M. S. Barker, P. G. Wolf, Unfurling Fern Biology in the Genomics Age. *Bioscience* **60**, 177–185 (2010). [doi:10.1525/bio.2010.60.3.4](https://doi.org/10.1525/bio.2010.60.3.4)
10. I. J. Leitch, A. R. Leitch, in *Plant Genome Diversity*, I. J. Leitch, J. Greilhuber, J. Doležel, J. F. Wendel, Eds. (Springer Verlag, Wien, 2013), vol. 2, pp. 307–322.
11. C. Augustsson, Lapilli tuff as evidence of Early Jurassic Strombolian-type volcanism in Scania, southern Sweden. *GFF* **123**, 23–28 (2001). [doi:10.1080/11035890101231023](https://doi.org/10.1080/11035890101231023)
12. See supplementary materials available on *Science* Online.
13. I. Bergelin, Jurassic volcanism in Skåne, southern Sweden, and its relation to coeval regional and global events. *GFF* **131**, 165–175 (2009). [doi:10.1080/11035890902851278](https://doi.org/10.1080/11035890902851278)
14. A. Ahlberg, U. Sivhed, M. Erlström, *Geol. Surv. Denm. Greenl. Bull.* **1**, 527–541 (2003).
15. S. D. Brack-Hanes, J. C. Vaughn, Evidence of paleozoic chromosomes from lycopod microgametophytes. *Science* **200**, 1383–1385 (1978). [Medline](#) [doi:10.1126/science.200.4348.1383](https://doi.org/10.1126/science.200.4348.1383)
16. K. J. Niklas, Differential preservation of protoplasm in fossil angiosperm leaf tissues. *Am. J. Bot.* **69**, 325–334 (1982). [doi:10.2307/2443136](https://doi.org/10.2307/2443136)
17. J. W. Hagadorn, S. Xiao, P. C. Donoghue, S. Bengtson, N. J. Gostling, M. Pawlowska, E. C. Raff, R. A. Raff, F. R. Turner, Y. Chongyu, C. Zhou, X. Yuan, M. B. McFeely, M.

- Stampanoni, K. H. Nealson, Cellular and subcellular structure of neoproterozoic animal embryos. *Science* **314**, 291–294 (2006). [Medline doi:10.1126/science.1133129](#)
18. A. E. DeMaggio, R. H. Wetmore, J. E. Hannaford, D. E. Stetler, V. Raghavan, Ferns as a model system for studying polyploidy and gene dosage effects. *Bioscience* **21**, 313–316 (1971). [doi:10.2307/1295880](#)
  19. J. Masterson, Stomatal size in fossil plants: Evidence for polyploidy in majority of angiosperms. *Science* **264**, 421–424 (1994). [Medline doi:10.1126/science.264.5157.421](#)
  20. I. Símová, T. Herben, Geometrical constraints in the scaling relationships between genome size, cell size and cell cycle length in herbaceous plants. *Proc. Biol. Sci.* **279**, 867–875 (2012). [Medline doi:10.1098/rspb.2011.1284](#)
  21. B. H. Lomax, J. Hilton, R. M. Bateman, G. R. Upchurch, J. A. Lake, I. J. Leitch, A. Cromwell, C. A. Knight, Reconstructing relative genome size of vascular plants through geological time. *New Phytol.* **201**, 636–644 (2014). [doi:10.1111/nph.12523](#)
  22. H. Hass, N. P. Rowe, in *Fossil Plants and Spores: Modern Techniques*, T. P. Jones, N. P. Rowe, Eds. (Geological Society, London, 1999), pp. 76–81.
  23. T. N. Taylor, M. Krings, N. Dotzler, J. Galtier, The advantage of thin section preparations over acetate peels in the study of Late Paleozoic fungi and other microorganisms. *Palaios* **26**, 239–244 (2011). [doi:10.2110/palo.2010.p10-131r](#)
  24. P. C. J. Donoghue, S. Bengtson, X. P. Dong, N. J. Gostling, T. Huldtgren, J. A. Cunningham, C. Yin, Z. Yue, F. Peng, M. Stampanoni, Synchrotron X-ray tomographic microscopy of fossil embryos. *Nature* **442**, 680–683 (2006). [Medline doi:10.1038/nature04890](#)
  25. E. M. Friis, P. R. Crane, K. R. Pedersen, S. Bengtson, P. C. Donoghue, G. W. Grimm, M. Stampanoni, Phase-contrast X-ray microtomography links Cretaceous seeds with Gnetales and Bennettitales. *Nature* **450**, 549–552 (2007). [Medline doi:10.1038/nature06278](#)
  26. M. D. Sutton, Tomographic techniques for the study of exceptionally preserved fossils. *Proc. Biol. Sci.* **275**, 1587–1593 (2008). [Medline doi:10.1098/rspb.2008.0263](#)
  27. K. Dybkjær, Palynological zonation and palynofacies investigation of the Fjerritslev Formation (Lower Jurassic–basal Middle Jurassic) in the Danish Subbasin. *Danm. Geol. Undersøg. Ser. A* **30**, 1–150 (1991).
  28. E. B. Koppelhus, L. H. Nielsen, Palynostratigraphy and palaeoenvironments of the lower to middle jurassic bagå formation of bornholm, denmark. *Palynology* **18**, 139–194 (1994). [doi:10.1080/01916122.1994.9989443](#)
  29. E. B. Koppelhus, G. Dam, *Geol. Surv. Denm. Greenl. Bull.* **1**, 723–775 (2003).
  30. J. J. Lund, K. R. Pedersen, *Bull. Geol. Soc. Den.* **33**, 371–400 (1985).
  31. W. D. Tidwell, *SIDA Contrib. Bot.* **16**, 253–261 (1994).
  32. Y.-M. Cheng, A new species of Ashicaulis (Osmundaceae) from the Mesozoic of China: A close relative of living Osmunda claytoniana L. *Rev. Palaeobot. Palynol.* **165**, 96–102 (2011). [doi:10.1016/j.revpalbo.2011.01.008](#)

33. N. Tian *et al.*, A specialized new species of *Ashicaulis* (Osmundaceae, Filicales) from the Jurassic of Liaoning, NE China. *J. Plant Res.* **127**, 209–219 (2014).
34. N. Tian *et al.*, *Sci. China Earth Sci.* 10.1007/s11430-013-4767-2 (2013).
35. S. Tappe, Mesozoic mafic alkaline magmatism of southern Scandinavia. *Contrib. Mineral. Petrol.* **148**, 312–334 (2004). [doi:10.1007/s00410-004-0606-y](https://doi.org/10.1007/s00410-004-0606-y)
36. G. Majno, I. Joris, Apoptosis, oncosis, and necrosis. An overview of cell death. *Am. J. Pathol.* **146**, 3–15 (1995). [Medline](#)